JCTC Journal of Chemical Theory and Computation

Article

pubs.acs.org/JCTC

Analytical Double-Hybrid Density Functional Based on the Polynomial Series Expansion of Adiabatic Connection: A Quadratic Approximation

Jaehoon Kim and Yousung Jung*

Graduate School of EEWS, Korea Advanced Institute of Science and Technology (KAIST), Daejeon 305-701, Republic of Korea

ABSTRACT: We present a systematic derivation of double-hybrid density functional (DHDF) based on the polynomial series expansion of adiabatic connection formula in the closed interval $\lambda = [0,1]$ without a loss of generality. Because of the tendency of W_λ having a small (but not negligible) curvature at equilibrium, we first evaluate the chemical validity of quadratic approximation for W_λ using the large GMTKN30 benchmark database. The resulting functional, obtained analytically and denoted by quadratic adiabatic connection functional-PT2 (QACF-2), is found to be robust and accurate (2.35 kcal/mol of weighted total mean absolute deviation error, WTMAD), comparable or slightly improved compared to other flavors of existing parameter-free DHDFs (2.45 or 3.29 kcal/mol for PBE0-2 or PBE0-DH, respectively). The nonlocal expansion coefficients obtained for the current QACF-2 ($a_{HF} = 2/3$, $a_{PT2} = 1/3$) also offer some interesting observation, in that the latter analytical coefficients are very similar to the empirically optimized coefficients in some of the best DHDFs today with high accuracy (1.5 kcal/mol). Effects of quadratic truncation in QACF-2 have been further assessed and justified by estimating the higher-order corrections to be as much as 0.54 kcal/mol. The present derivation and numerical experiments suggest that the quadratic λ dependence, despite its simplicity, is a surprisingly good approximation to the adiabatic connection that can serve as a good starting point for further development of accurate parameter-free density functionals.

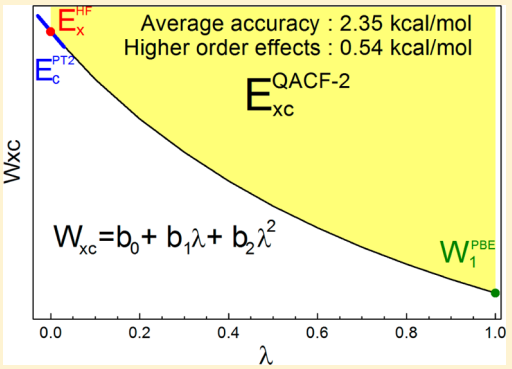

I. INTRODUCTION

The Kohn−Sham (KS) decomposition of density functional theory (DFT)[1] has been widely used as a cost-effective electronic structure method to calculate molecules and materials. It assumes a mapping in which the ground-state electron density of the noninteracting system is equal to that of the real system, and, hence, one only needs to solve an associative single particle equation, instead of a many-body equation. The KS electronic energy is defined as

$$E = T_s + J + V_{ext} + E_{xc} \quad (1)$$

where T_s and J are the noninteracting kinetic and coulombic energies that are used to approximate those of the real system, V_{ext} is the energy due to the external potential such as nuclei, and E_{xc} is the sum of exchange and correlation energy plus the remaining missing effects due to the noninteracting approximation of the kinetic energy. While the existence of exact density functional has been proven,[2] the programmable method for the exact theory is not well-established. Some practical approximations to E_{xc} include local density approximation (LDA) and generalized gradient approximation (GGA) within the KS formalism. However, the predictive power of these conventional approximations is, in many cases, poor, particularly for molecular systems where the electron density changes rapidly as a function of distance. For example, the accuracy of thermochemical properties of LDA and GGA that describe the bonding characteritics of molecules are not near quantitative (far greater than the chemical accuracy 1 kcal/mol for atomization energies relative to experiments) and weak intermolecular interactions are often incorrect, even qualitatively.[3]

Hybrid functionals improve the descriptions of molecular properties by including the interactions among the occupied KS-orbitals, namely, by adding the Hartree−Fock (HF)-like exact exchange terms. Becke[4] first gave a theoretical justification to mix in this nonlocal HF term to improve the accuracy by using the adiabatic connection (AC) formula,[5−7]

$$E_{xc} = \int_0^1 W_\lambda \, d\lambda \quad (2)$$

$$W_\lambda = \langle \Psi_\lambda | \hat{V}_{ee} | \Psi_\lambda \rangle - J \quad (3)$$

where λ is the coupling parameter that controls the strength of electron−electron interaction and W_λ is the exchange and correlation energy at a given interaction strength λ. We note that W_λ itself does not contain the correlation effects from kinetic energy, but after integration over λ, the kinetic part of the correlation energy is recovered in E_{xc}. This formula might be misused if W_λ is not defined carefully, since it is different from E_{xc}, in terms of kinetic correlation.

Received: March 28, 2014

dx.doi.org/10.1021/ct500660k | J. Chem. Theory Comput. XXXX, XXX, XXX−XXX

Becke used a simple linear interpolation for W_λ as a function of λ, and approximated W_λ at $\lambda = 1$ (fully interacting limit) by LDA[8] while utilizing the fact that W_λ at $\lambda = 0$ (noninteracting limit) equals the exchange energy of the KS wave function. As a result, the first hybrid functional, namely, the half-and-half (H&H) functional,[4] was obtained:

$$E_{xc}^{H\&H} = \frac{1}{2}E_x^{HF} + \frac{1}{2}W_1^{LDA} \tag{4}$$

where W_λ^{LDA} denotes the local density approximations to exchange and potential-correlation, and E_x^{HF} is the HF-like exchange using KS orbitals. Becke's H&H functional can be seen as connecting the "exact" exchange from the Hartree–Fock theory and density functional correlation energy from DFT with a mathematically well-defined way, and it has been shown to significantly reduce the errors of many molecular properties in practice indeed (atomization energy, ionization potential (IP), and proton affinity (PA)). In fact, many regard that this derivation of the hybrid functional and demonstration of its chemical performance was a turning point where DFT began to be routinely used to describe molecules in chemistry, extending substantially the applicability of LDA and GGA-based DFT that was already quite successful to describe solids.

More generally, a density functional approximation (DFA) to W_λ^{DFA} can be obtained from the exchange and correlation functional via the coordinate scaling:[9,10]

$$W_\lambda^{DFA} = \frac{\partial}{\partial\lambda}\{\lambda^2 E_{xc}^{DFA}[\rho_{1/\lambda}]\} \tag{5}$$

where $\rho_{1/\lambda}(r) = \lambda^{-3}\rho(r/\lambda)$ is the scaled electron density. Although λ in eq 2 denotes the strength of electron–electron interactions and λ in $\rho_{1/\lambda}(r)$ of eq 5 denotes the coordinate scaling, these two λ parameters are related, since the coordinate scaling of the Hamiltonian and its ground state wave function (as well as density) can be interpreted as a result of modifying the strength of electron–electron interactions. Therefore, the scaled Hamiltonian leads to the modified electron–electron interaction energy for a given coupling strength, and the AC formula can be derived from the coordinate scaling relation, as in eq 5.

Later, other derivations of hybrid functional such as PBE0,[11] two-legged functional,[12] and MCY[13] were proposed based on adiabatic connection. PBE0 was obtained from a simple adiabatic connection model, made by adding a simple correction ansatz to the original PBE model,

$$W_\lambda^{PBE0} = W_\lambda^{PBE} + (E_x^{HF} - E_x^{PBE})(1-\lambda)^3 \tag{6}$$

The third-order polynomial in λ in eq 6 (or fourth-order in λ after integration) was interpreted as fourth-order correction term in perturbation theory (MP4) that captures most of the correlation effects for molecules. The last term in eq 6, its gradient, and the second-order gradient all vanish at $\lambda = 1$ by construction, to utilize the fact that W_λ^{DFA} is most reliable at $\lambda = 1$, because of the rapid variation of density gradient for the scaled density. For the $\lambda = 0$ noninteracting limit, the PBE0 also recovers the exact exchange as in H&H.

The two-legged functional is made from two partial linear approximations of the adiabatic connection, so the geometric shape of W_λ is the two straight line segments connected together, as a function of coupling parameter. The meeting point of the two line segments was chosen such that the area under the two-legged curve is simply the energy at which the two legs meet. The hybrid version of the latter approach by assuming the $\lambda = 0$ limit to be the exact exchange yielded the improved description for the multiple-bonded molecules.

The MCY functional adopted a nonpolynomial model, the [1,1] Padé expansion form for the λ-dependence of adiabatic connection curve that includes three parameters. The authors used a set of three conditions to solve for the three parameters: W_0, W_λ, and $dW_\lambda/d\lambda$ at $\lambda = 0$. In particular, the slope at $\lambda = 0$ was taken from the modified TPSS functional to ensure the self-interaction-free condition for the one-electron system, scaled empirically with the factor of 4.0 to further enhance the chemical performance of the functional. Density functional approximation to W_λ was made by the BLYP functional, with the location of λ optimized to 0.6–0.7, based on chemical tests. This MCY functional is a self-interaction-free functional by construction, and it is hybrid meta-GGA functional from the AC model.

Attempts to include the nonlocal part of correlation energy via perturbative approach, in addition to the nonlocal exchange, have then appeared with the name, double hybrid density functional (DHDF).[14−32] In this approach, not only the interactions between occupied orbitals, but also the interactions between the occupied and virtual orbitals are also included to describe the nonlocal correlation effects, in a manner similar to second-order Mollet-Plesset perturbation theory (MP2). Many DHDFs have been proposed but take, more or less, a standard form:[15,18,33]

$$E_{xc}[\rho] = a_x E_x^{HF} + (1-a_x)E_x^{DFA} + (1-a_c)E_c^{DFA} + a_c E_c^{PT2} \tag{7}$$

where E_c^{PT2} is a perturbation term whose mathematical expression is identical to MP2 but evaluated with the KS orbitals. Equation 7 uses two mixing parameters a_x and a_c, but there can be more parameters depending on the construction.[14,17,19−21,23−27,34] Though the double-hybrids described above have provided high accuracy on a wide range of chemical properties, they do not fully capture the long-range van der Waals interactions.[34−36] To remedy this, range-separated MP2 correlation correction[17,19] and empirical long-range dispersion correction[16] have also been suggested. It is also possible to incorporate the idea of spin-component scaled MP2 or scaled opposite-spin MP2 methods into DHDFs, such as in B2-O3LYP[17] or XYGJ-OS.[26] By combining all these ingredients, perhaps the most sophisticated empirical double-hybrid functional can take the form as in eq 8, that is, dispersion-corrected, spin-component scaled[37] double hybrid functional (DSD-DFT).[23,34] In DSD-DFT, the sum of correlation coefficients generally are not unity.

$$E_{xc}[\rho] = a_x E_x^{HF} + (1-a_x)E_x^{DFA} + a_c E_c^{DFA} + a_s E_c^{SS\text{-}PT2} + a_o E_c^{OS\text{-}PT2} + c_6 E_D \tag{8}$$

A more rigorous theoretical justification for DHDF was given later using the scaling relation of exchange and correlation,[21,24,25,27] as well as different two-point linear interpolations of adiabatic connection formula.[20,26] In particular, the fact that the first derivative of W_λ at $\lambda = 0$ is equal to the second-order terms from the Görling–Levy perturbation theory (GL2),[38] provided the key motivation to include the nonlocal E_c^{PT2} terms in eq 7. The latest DHDFs thus designed are indeed shown to offer high accuracy (1.5–2.5 kcal/mol error for atomization energies) for van der Waals interactions, as well as thermochemical performance. Nonetheless, many of these

dx.doi.org/10.1021/ct500660k | J. Chem. Theory Comput. XXXX, XXX, XXX–XXX

present and, in particular, those DHDFs that perform chemically very well, are based on the empirical fitting of the expansion coefficients in eq 7 or eq 8 to the known experimental or highly accurate ab initio data.

There also have been some efforts to develop several parameter-free DHDFs.[21,27,30,31] In PBE0-DH[21] and PBE0-2,[27] the authors essentially assumed the linearly scaled one-parameter double hybrid approximation (LS1DH)[25] in which the density scaling in the correlation functional takes the linear approximation, namely, $E_c[\rho_{1/\lambda}] = \lambda E_c[\rho] + (1 - \lambda)E_c^{GL2}[\rho]$, yielding the one-parameter condition $a_c = a_x^3$ via eq 5. Therefore, to determine the remaining one parameter, a_x or a_c in eq 7 PBE0-DH utilized the averaged exchange mixing between HF-like and PBE exchanges ($a_x = 0.5$), whereas PBE0-2 used the averaged correlation mixing between MP2-like and PBE correlations ($a_c = 0.5$). More recently, Su and Xu reported another parameter-free double hybrid functional from adiabatic connection (called ACDH).[31] They considered the zero and infinite electron−electron interaction energies and adiabatic connection in these limits to construct the nonlinear AC formula. This nonlinear ACDH ansatz includes two system-dependent parameters, but these were determined by the near-linearity assumption of the AC curve for molecules at equilibrium as in the Becke's H&H model, giving $a_x = 0.5$ with $a_c = 0.1151$. The G3/99 benchmark test for the heats of formation showed the better performance of PBE-ACDH (3.5 kcal/mol), compared to previous PBE0-DH (5.1 kcal/mol) and PBE0-2 (5.2 kcal/mol).

As shown in this brief overview on the development of DHDFs in the literature, the adiabatic connection formula has been quite useful to derive accurate, parameter-free, or theoretically more justifiable functionals, but mainly based on the 50:50 average mixing. In this paper, we generalize and offer a theoretical justification of using polynomial series expansion for W_λ when the desired E_{xc} is a linear combination of several existing functionals, and then show by numerial experiments that the quadratic truncation is a very good approximation for DHDFs for chemical applications. That is, the simple parameter-free quadratic adiabatic connection functional-PT2 (QACF-2) yields the weighted mean absolute deviation error of 2.35 kcal/mol for the extensive GMTKN30 database, a remarkable accuracy considering that no parametrization is involved, similar to the accuracy of some of the best optimized DHDFs with three and more parameters.[39] We also estimate the effects of including higher-order corrections beyond the quadratic approximation to be 0.54 kcal/mol, again justifying the quadratic approximation. Potential further implications of our results toward the development of accurate density functionals in a more systematic manner are discussed.

II. THEORY

In this section, we show that any density functional that takes the linear combination of various components (mostly existing exchange and correlation functionals) can be generally constructed from the polynomial approximation of the adiabatic connection function, W_λ. For adiabatic connection curve, i.e., the dependence of W_λ on λ in eq 3, many mathematical forms[11−13,40−46] have been studied. Many of these models are usually constructed to satisfy the monotonic decrease condition on W_λ throughout all λ, the exact exchange condition on W_0 for the Kohn−Sham noninteracting limit, and the derivative condition of W_λ at $\lambda = 0$ being equal to the GL2 term. If the adiabatic connection model (W_λ) is nonlinear, with respect to the parameters, then the integrated exchange correlation functional (E_{xc}) is also nonlinear.[13,40−42,45] Particularly relevant to the present approach are the seminal works by Yang and co-workers[41] and Tozer and co-workers,[40,45] which used the same quadratic equation to approximate W_λ in the end. Below, we offer a theoretical justification of using this quadratic expression of adiabatic connection, and we comment on the differences between those results obtained in the works by Yang and co-workers[41] and Tozer and co-workers,[40,45] and the present results.

In this work, we begin with an ansatz that the desired functional (E_{xc}) is a linear combination of several ingredients. The general expression for the adiabatic connection function that meets this constraint is

$$W_\lambda = \sum_i a_i f_i(\lambda) \tag{9}$$

where the expansion coefficients a_i are determined by W_λ or its derivatives at carefully chosen λ values (typically 0 or 1, or can be many more). Since any continuous function $f_i(\lambda)$ can be approximated by polynomials to any accuracy in the closed interval $\lambda = [0,1]$ (Weierstrass approximation theorem),[47,48] we can rewrite W_λ as a polynomial expansion without a loss of generality:

$$W_\lambda = \sum_{i\geq 0} b_i\lambda^i = b_0 + b_1\lambda + b_2\lambda^2 + \sum_{i>2} b_i\lambda^i \tag{10}$$

We note that this polynomial expansion is the most general expression under the constraint described above, although more-general nonlinear expansion forms have already been studied.[13,40−42,45] Furthermore, this polynomial expansion can still treat a difficult case such as H_2 molecules in the dissociation limit, since the Weierstrass approximation theorem is generally applicable to W_λ itself, as long as W_λ is continuous. To analytically determine the expansion coefficients up to nth order, one must have $n + 1$ known or approximate conditions. Here, we use the following three conditions at $\lambda = 0$ and 1 as given in the literature:[11,20,26]

$$W_0 = E_x^{HF} \tag{11}$$

$$W_1 \approx W_1^{DFA} \tag{12}$$

$$W_0' = \left[\frac{dW}{d\lambda}\right]_{\lambda=0} = 2E_c^{GL2} \approx 2E_c^{PT2} \tag{13}$$

Equation 12 is a good approximation since W_λ^{DFA} is most reliable at $\lambda = 1$ for typical LDA or GGA,[11] and negligible singles contribution of GL2 term yields eq 13. If we truncate the expansion at nth order in λ ($n > 2$) and utilize eqs 11−13, there are $n - 2$ free parameters that must be further determined, for example, by imposing additional conditions or fitting to the experimental or training benchmark database. For quadratic ($n = 2$) and cubic ($n = 3$) truncations; therefore, we obtain the exchange correlation energy expression as in eqs 14 and 15, for example. Adding additional higher-order terms will only increase the number of free parameters such as b_4, b_5, etc. in a form similar to eq 15.

$$E_{xc}(n = 2) = \frac{2}{3}E_x^{HF} + \frac{1}{3}W_1^{DFA} + \frac{1}{3}E_c^{PT2} \tag{14}$$

$$E_{xc}(n = 3) = \frac{2}{3}E_x^{HF} + \frac{1}{3}W_1^{DFA} + \frac{1}{3}E_c^{PT2} - \frac{1}{12}b_3 \tag{15}$$

dx.doi.org/10.1021/ct500660k | J. Chem. Theory Comput. XXXX, XXX, XXX−XXX

Table 1. Weighted Mean Absolute Deviation Errors for the GMTKN30 Benchmark Set for LDA, GGA, Hybrid, and Double-Hybrid Functionals[a]

	Mean Absolute Deviation Error (kcal/mol)										
dataset[b]	PBE	B3LYP	PBE0	XYG3	XYGJ-OS	B2PLYP	DSD-BLYP	PBE0-DH	PBE0-2	QACF-2	MP2[c]
MB08-165	9.18	7.27	8.75	4.40	2.72	4.38	3.15	8.38	4.33	4.69	5.72
W4-08	13.03	3.84	3.92	2.86	2.45	2.98	4.32	6.50	5.85	10.40	8.71
G21IP	3.73	3.85	3.74	1.40	1.37	2.49	2.03	3.19	2.47	3.16	3.44
G21EA	2.42	2.30	3.02	2.01	1.84	2.14	2.60	3.43	2.95	3.80	2.83
PA	2.01	2.17	1.95	1.57	1.15	1.50	1.21	2.44	1.16	1.55	1.38
SIE11	10.27	8.50	8.48	3.65	3.00	6.23	4.73	5.28	3.99	4.01	4.56
BHPERI	3.08	5.55	2.03	1.66	3.50	2.24	1.29	1.84	2.48	1.55	6.17
BH76	9.03	4.53	3.98	1.04	1.04	2.43	1.03	1.56	2.07	1.17	4.36
BH76RC	4.25	2.06	2.35	1.12	0.97	1.10	1.04	2.23	2.06	1.53	3.65
RSE43	3.52	2.39	2.02	0.66	0.51	1.28	0.71	1.13	0.84	0.64	3.16
O3ADD6	4.40	2.10	5.17	2.84	3.72	2.30	2.27	5.19	3.14	2.40	5.65
G2RC	5.98	2.87	6.67	2.54	1.98	2.16	2.81	7.50	5.92	4.81	3.59
AL2X	4.36	7.80	2.20	0.81	0.86	2.34	0.79	0.94	2.50	0.99	2.91
NBPRC	2.65	4.48	2.63	0.66	0.56	2.16	0.61	2.68	2.88	0.84	1.51
ISO34	1.79	2.18	1.72	1.10	0.69	1.25	0.95	1.72	1.51	1.06	1.59
ISOL22	6.39	9.98	4.41	3.03	2.23	4.50	1.88	1.99	1.19	1.86	1.87
DC9	13.15	13.38	11.62	3.67	2.69	5.22	4.78	9.57	8.43	7.28	11.32
DARC	6.03	14.38	3.03	1.00	0.81	6.87	1.48	5.88	8.55	2.67	3.95
ALK6	1.60	3.30	3.26	2.29	2.12	1.33	3.49	3.75	4.45	1.64	8.16
BSR36	6.41	9.01	6.43	0.33	1.28	2.62	3.51	3.46	2.82	0.78	4.08
IDISP	8.69	13.62	6.76	1.08	1.88	6.25	3.30	6.10	1.58	2.60	4.60
WATER27	4.71	4.18	3.32	2.97	4.94	1.91	6.23	3.06	3.54	2.15	1.39
ADIM6	3.24	4.90	2.76	0.88	0.91	2.12	0.56	2.37	0.76	1.91	0.27
PCONF	3.55	3.61	3.18	0.31	0.28	1.62	0.68	1.84	0.32	1.07	0.19
ACONF	0.53	0.89	0.53	0.12	0.11	0.55	0.31	0.33	0.07	0.23	0.08
SCONF	0.34	0.78	0.39	0.08	0.12	0.41	0.24	0.25	0.18	0.30	0.16
CYCONF	0.82	0.43	0.54	0.24	0.14	0.25	0.13	0.34	0.22	0.10	0.22
S22	2.28	3.39	1.97	0.22	0.38	1.44	1.16	1.17	0.69	0.53	0.98
WTMAD (all)	**5.21**	**4.68**	**3.77**	**1.51**	**1.37**	**2.36**	**1.85**	**3.29**	**2.45**	**2.35**	**3.14**
MUE (all)	**4.91**	**5.13**	**3.82**	**1.59**	**1.58**	**2.57**	**2.05**	**3.35**	**2.77**	**2.35**	**3.45**
RMSD (all)	**6.05**	**6.37**	**4.67**	**2.09**	**1.98**	**3.23**	**2.69**	**4.17**	**3.54**	**2.95**	

[a]All calculations are performed using the 6-311+G(3df,2p) basis unless noted otherwise. [b]Legend: MB08-165 (decomposition energies of 165 randomly created molecular systems), W4-08 (atomization energies of small molecules), G21IP (adiabatic ionization potentials), G21EA (adiabatic electron affinities), PA (adiabatic proton affinities), SIE11 (self-interaction error related problems), BHPERI (barrier heights of pericyclic reactions), BH76 (barrier heights of hydrogen transfer, heavy atom transfer, nucleophilic substitution, unimolecular, and association reactions), BH76RC (reaction energies of the BH76 set), RSE43 (radical stabilization energies), O3ADD6 (reaction energies, barrier heights, association energies for addition of O_3 to C_2H_4 and C_2H_2), G2RC (reaction energies of selected G2/97 systems), AL2X (dimerization energies of AlX_3 compound), NBPRC (oligomerization and H_2 fragmentations of NH_3/BH_3 systems; H_2 activation reactions with $PH3/BH_3$ systems), ISO34 (isomerization energies of small and medium-sized organic molecules), ISOL22 (isomerization energies of large organic molecules), DC9 (9 different cases for DFT), DARC (reaction energies of Dials-Alder reactions), ALK6 (fragmentation and dissociation reactions of alkaline and alkaline-cation-benzene complexes), BSR36 (bond separation reactions of saturated hydrocarbons), IDISP (intramolecular dispersion interactions), WATER27 (binding energies of water, $H^+(H_2O)_n$ and $OH^-(H_2O)_n$ clusters), PCONF (relative energies of phenylalanyl−glycyl−glycine tripeptide conformers), ACONF (relative energies of alkane conformers), SCONF (relative energies of sugar conformers), CYCONF (relative energies of cysteine conformers), S22 (binding energies of noncovalently bound dimers), ADIM6 (interaction energies of *n*-alkane dimers). [c]MP2 data is taken from ref 39 and based on the CBS extrapolation using the def2-(TQ)ZVPP basis sets.

In order to keep the functional within the framework of double hybrid functional without introducing additional functional ingredients or conditions, we assume that the set of higher-order b_i parameters ($i > 2$) should all be a linear combination of W_0, W_1, and W_0'. This then leads to a simple expression that includes the higher-order effects as

$$E_{xc}(n=\infty) \approx \left(\frac{2}{3}+c_0\right)E_x^{HF} + \left(\frac{1}{3}+c_1\right)W_1^{DFA} + \left(\frac{1}{3}+c_2\right)E_c^{PT2} \quad (16)$$

The c_i terms are the free parameters that represent the higher-order correction effects. Essentially, by a simple scaling of the coefficients in eq 16, one can further optimize the functional given the choice of W_λ that includes the higher-order effects. Of course, if the optimal (c_0, c_1, c_2) turn out to be (0, 0, 0) or close to it, it would mean that the quadratic approximation of adiabatic connection is near optimal, given the choice of W_λ.

As we noted previously, the quadratic expression given in eq 14 was first considered by Yang and co-workers[41] and Tozer and co-workers,[40,45] but the key difference is that, to determine the expansion coefficients, these authors used $W_{\lambda_p=0.63} \approx$

dx.doi.org/10.1021/ct500660k | J. Chem. Theory Comput. XXXX, XXX, XXX−XXX

$W^{BLYP}_{\lambda_p=0.63}$ and $W'_0 = 4W'^{BLYP}_0$,[41] or used the full CI density to evaluate W_0, W_1, and W'_0.[40,45] The quadratic model of Yang and co-workers yielded the mean absolute error of 6.60 kcal/mol for 407 atomization energies, but Tozer's model (denoted as the AC3 model) was applied only to two-electron systems and has not been benchmarked for general chemical performance, because of the use of full CI calculations.

III. BENCHMARK EVALUATION AND DISCUSSION

Computational Details and Notations. The key expressions that we will use and evaluate in this paper are eq 14 (quadratic approximation) and eq 16 (adding higher-order corrections beyond quadratic truncation), incorporating the conditions in eqs 11−13. In eq 13, we replace E_c^{GL2} by E_c^{PT2}, as in most double hybrid literature, neglecting the singles contribution, where E_c^{PT2} is a perturbation term whose mathematical expression is identical to MP2 but evaluated with the KS orbitals. The only remaining task is then the choice of density functional approximation in W_1^{DFA} and the choice of Kohn−Sham orbitals to evaluate eq 14. In this work, we explored PBE to approximate W_1^{DFA}. For the choice of orbitals, ideally, one would like to use the total energy expression in eq 14 to get the relaxed orbitals under the full correlation field as in the orbital optimized double-hybrid functionals recently reported,[30] but only with increased computational cost. So, instead, here we used the orbitals obtained self-consistently from eq 14 excluding the PT2 part as in many existing DHDFs.[15−21,23,24,26−28,32−34] We denote the latter method of choice as quadratic adiabatic connection functional-PT2 (QACF-2).

We performed the extensive benchmark test for QACF-2 with the GMTKN30 (General Main group Thermochemistry, Kinetics, and Noncovalent interactions) database,[39,49] which includes thermochemistry, kinetics, self-interaction errors (SIEs), electron affinity (EA), IP, PA, noncovalent interaction, isomerization energies, etc. (a total of 841 molecular systems). To summarize all the statistics, a statistic called "weighted total mean absolute deviation" (WTMAD)[39] is calculated as a weighted sum of those:

$$\mathrm{WTMAD} = \frac{\sum_i w_i \times \mathrm{MAD}_i}{\sum_i w_i} \tag{17a}$$

$$w_i = N_i \times \frac{\mathrm{MAD}_i^{\mathrm{BLYP}}}{\mathrm{MAD}_i^{\mathrm{B2PLYP\text{-}D}}} \tag{17b}$$

where N_i is the number of entries of each subset. The WTMAD was constructed to give more weights to the difficult molecular systems, using the ratio between the mean absolute deviations (MAD) of BLYP and B2PLYP-D. To test the adequacy of using WTMAD as a statistical error measure, we also used more-traditional measures, such as root-mean-square deviation (RMSD) or mean unsigned error (MUE). The RMSD was calculated by computing the RMSD value for each subset and taking the average of the RMSDs of all 28 subsets, and similarly for MUE also. The subsets including heavy atoms (RG6, HEAVY28) were not included here, because the 6-311+G-(3df,2p) basis set (which was used for the benchmark tests) is not supported for those atoms. We implemented QACF-2 in a development version of Q-Chem.[50] We compare the performance of QACF-2 against some representative and the parent functionals of QACF-2 in Table 1; GGA (PBE), hybrid GGA (B3LYP and PBE0), parametrized (XYG3, XYGJ-OS, B2PLYP, DSD-BLYP) and parameter-free double hybrid functional (PBE0-DH, PBE0-2), and a related wave function method with the same cost (MP2) in Table 1. The basis set superposition error (BSSE) correction is not applied to all benchmark calculations.

Benchmark Results of Quadratic Approximation. The WTMAD error of QACF-2 is 2.35 kcal/mol, which is very close to some of the most accurate DHDFs tested in this work, such as B2PLYP[15] (2.36 kcal/mol), XYG3[20] (1.51 kcal/mol), or XYGJ-OS[26] (1.37 kcal/mol). QACF-2 generally performs well for reaction barriers and reaction energies, as well as noncovalent interactions. These accuracies for QACF-2 are rather remarkable, considering that there are no fitting parameters involved and all the expansion coefficients are analytically derived based on the adiabatic connection. Compared to other parameter-free DHDFs, QACF-2 (2.35 kcal/mol) show improved statistical results (3.29 kcal/mol for PBE0-DH, and 2.45 kcal/mol for PBE0-2) using the 6-311+G(3df,2p) basis. The result in Table 1 also indicate that there is a slight variation in the calculated error values using RMSD or MUE, but the relative accuracy ranking of all seven double-hybrid methods considered here is unaltered, using three different statistical measures of errors (WTMAD, RMSD, and MUE).[36]

Because of an important application area of DHDFs for noncovalent interactions, in particular, we further analyzed the performance of QACF-2 for the S66 × 8 database,[51] which can be partitioned into dispersion- and electrostatics-dominant systems, as well as systems including both types of noncovalent interactions. The total MAD of QACF-2 for S66 × 8 (0.51 kcal/mol) is similar to that for S22 (0.53 kcal/mol). For electrostatic-dominant systems (blue lines in Figure 1), the overall error is 0.19 kcal/mol, with almost even distributions for the overbinding and underbinding cases (i.e., without systematic trend). For dispersion-dominant systems (red lines in Figure 1), however, almost all cases (210 cases out of 216) underbind, suggesting that QACF-2 has an inherent and systematic deficiency of describing dispersion interactions. Considering that we did not correct for the basis set superposition error (BSSE) in these benchmark calculations while applying 6-311+G(3df,2p), a moderate basis set for PT2 calculations, we expect that the latter underbinding of QACF-2

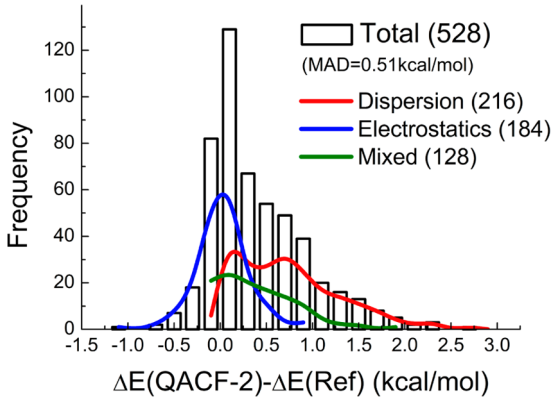

Figure 1. Relative error histogram of QACF-2, compared to reference CCSD(T)/CBS for S66 × 8 benchmark database. The 6-311+G-(3df,2p) basis set was used. The numbers in parentheses indicate the sample sizes.

dx.doi.org/10.1021/ct500660k | J. Chem. Theory Comput. XXXX, XXX, XXX−XXX

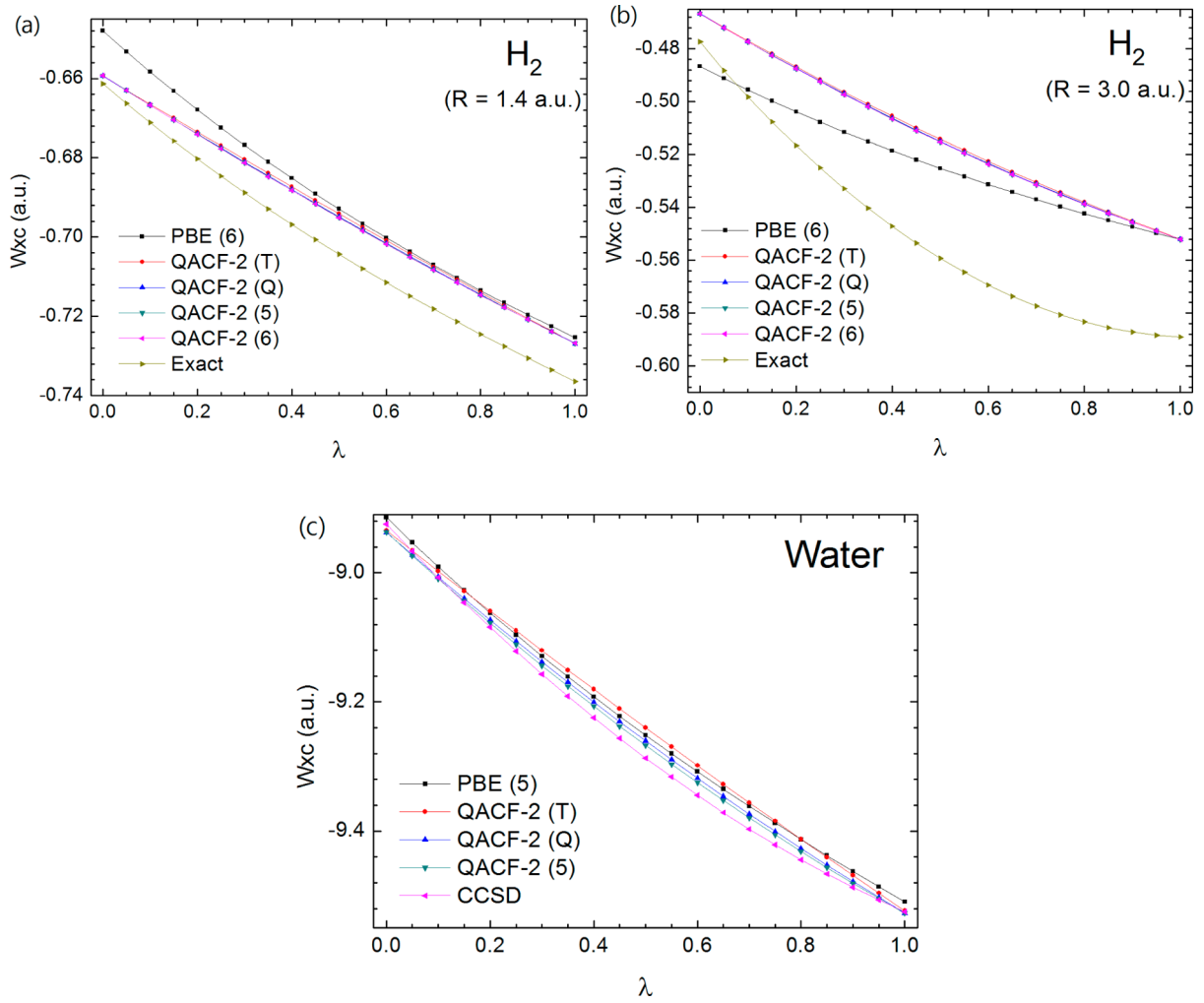

Figure 2. Assumed adiabatic connection curves for (a) the H_2 molecule at near-equilibrium, (b) the stretched H_2 molecule, and (c) the water molecule for PBE, QACF-2 functionals. The aug-cc-PVxZ basis are abbreviated as (x) in legends, and CCSD or exact curves are taken from ref 42.

will worsen for van der Waals complexes if the BSSE counterpoise correction is applied, perhaps not surprising due to the inclusion of only 30% of the PT2 correlation term. For the same reason, the larger PT2 portion of another parameter-free DHDF, PBE0-2 (50% PT2), makes PBE0-2 perform better for the vdW systems than QACF-2. For example, for the IDISP subset, PBE0-2 and QACF yields the error of 1.58 kcal/mol vs 2.60 kcal/mol, respectively.

To understand the nature of high accuracy of QACF-2, we compared the quadratic adiabatic connection curves with the exact or coupled-cluster AC curves for two small molecules: H_2 and water. The full-CI and CCSD AC curves for the equilibrium H_2 and water molecules, respectively, were previously shown to have a very small curvature (almost linear but not negligible) inside the region $\lambda = [0,1]$,[40,42,45] suggesting that the present quadratic approximation might also be a good approximation. The calculated quadratic AC curves ($W_c = W_\lambda - W_0$) for the equilibrium H_2 and water molecules are reasonably close to the reference full-CI or CCSD AC curves at equilibrium, supporting the quadratic approximation for these systems.

The main discrepancies in the computed AC curves, however, arise from the initial slope that is underestimated in QACF-2 and the conventional DFA approximation at $\lambda = 1$. Although increasing the basis set (from aug-cc-pVDZ to aug-cc-pV6Z) improves the initial slope of QACF-2 slightly, a noticeable difference still exists between the PT2 slope and the exact slope using FCI. The latter difference, we show, is due to the use of KS orbitals obtained self-consistently from eq 14, excluding the PT2 part. In fact, for any DHDF that includes the positive portion of the PT2 term, the orbitals obtained using the truncated hybrid part always underestimate the PT2 term, compared to the fully relaxed KS orbitals. Using a variational principle, one can write

$$E^{\mathrm{DHDF}}[\Psi^{\mathrm{SCF}}] > E^{\mathrm{DHDF}}[\Psi^{\mathrm{rlx}}] \tag{18a}$$

$$E^{\mathrm{DHDF}}[\Psi^{\mathrm{SCF}}] - a_{\mathrm{PT2}}E_c^{\mathrm{PT2}}[\Psi^{\mathrm{SCF}}] < E^{\mathrm{DHDF}}[\Psi^{\mathrm{rlx}}] - a_{\mathrm{PT2}}E_c^{\mathrm{PT2}}[\Psi^{\mathrm{rlx}}] \tag{18b}$$

where Ψ^{SCF} and Ψ^{rlx} stand for self-consistent orbitals using eq 14, excluding the PT2 part and fully relaxed KS orbitals including the PT2 field, respectively, and E^{DHDF} is the total DHDF energy, such as eq 14. From eqs 18a and 18b, we then have

$$E_c^{\mathrm{PT2}}[\Psi^{\mathrm{SCF}}] > E_c^{\mathrm{PT2}}[\Psi^{\mathrm{rlx}}] \tag{18c}$$

indicating that the initial slope of DHDF using "truncated" orbitals would always underestimate the correct slope. Thus, it can be expected that the orbital-optimized double hybrid

dx.doi.org/10.1021/ct500660k | J. Chem. Theory Comput. XXXX, XXX, XXX−XXX

approach[30] to QACF-2 would improve the accuracy of the PT2 term and the energy value itself.

The quadratic polynomial is, by definition, not automatically guaranteed to have the monotonicity condition of the AC curve. However, when we tested the monotonicity for the entire GMTKN30 database that we considered in this work (~1200 molecules, including equilibrium and transition states), we found no case that violates the monotonicity. The condition to ensure the monotonicity of the integrand is a negative gradient of W_λ at $\lambda = 1$:

$$b_1 + 2b_2 < 0 \tag{19a}$$

$$E_x^{HF} + E_c^{PT2} > W_1^{DFA} \approx E_{xc}^{DFA} + E_c^{DFA} \tag{19b}$$

Equation 19a may be rearranged to read as eq 19b. In the literature, the W_λ^{DFA} terms have an almost linear form,[42] so W_λ^{DFA} can be approximately viewed as $W_1^{DFA} \approx E_x^{DFA} + 2E_c^{DFA} = E_{xc}^{DFA} + E_c^{DFA}$. Therefore, the last additional correlation term is perhaps responsible for our observation that monotonicity was always met in practice, at least for the present cases.

For all 1218 molecules considered here, the average deviation of the calculated AC curve from the linearity was 0.25% (R^2 = 0.9975). These results are in agreement with the analytical proof of Levy and Perdew that the W_λ curve of the ground state must be almost linear for any neutral molecular system.[9] However, since the systems with strong static correlation would deviate more from linearity, such as in the transition-state structures, the good performance of QACF-2 for barrier heights may indicate some cancellation of errors in practice. Indeed, in Figure 2b, for stretched H_2, the QACF-2 AC curve deviates more from the exact AC curve.

Basis Set Dependence. The choice of basis set affects the accuracy in practice. It is widely known that the MP2 term, just like any other correlated methods, has a slow basis set convergence.[52] Because of this, many existing DHDFs, such as B2PLYP,[15] B2T-PLYP,[18] B2K-PLYP,[18] B2GP-PLYP,[33] and DSD-DFTs,[23,34] are indeed developed with very large basis sets involving quadruple- or quintuple-ζ basis sets, although triple-ζ basis sets were also used in some DHDFs, such as wB97X-2 (LP),[19] XYG3,[20] and XYGJ-OS[26] for practical advantages. The basis set sensitivity of DHDFs on the chemical performance is clear, because of the inclusion of the PT2 term; however, it is unclear[20,39,53,54] whether the results always get improved with increasing basis set quality, since these empirical DHDFs are parametrized with a particular basis set chosen, and, hence, the basis set employed in the optimization might also be regarded as one such fitting parameter.[53,54]

For parameter-free DHDFs considered here, on the other hand, it is an interesting question whether increasing the basis set size would yield systematically improved accuracy, since, for these nonempirical DHDFs, there is no such optimization procedure in which the basis set is one of the optimization inputs. Therefore, we tested the basis set dependence of three nonempirical DHDFs (PBE0-DH, PBE0-2, and QACF-2) on the six subsets of GMTKN30, namely, MB08-165, W4-08, BH76, BSR36, S22, and CYCONF. These subsets were chosen as a representative of chemical interactions (MB08-165, W4-08, BH76, and BSR36) and noncovalent interactions (S22 and CYCONF): six subsets that have the largest weights w_i in eqs 17. We used def2-TZVPP and def2-QZVP basis sets. The results are summarized in Table 2. The present evaluation of the basis set dependence is certainly a brief test of using only two sets of basis sets, triple-ζ vs quadruple-ζ of the Ahlrich's type; hence, a more systematic and detailed test would be helpful in the future, but it is clear that the accuracy does improve consistently when going from def2-TZVPP to def2-QZVP for all three parameter-free DHDFs, by 0.20−0.58 kcal/mol.

Table 2. Basis Set Dependence of the Parameter-Free DHDFs, PBE0-DH, PBE0-2, and QACF-2, for the Six Subsets of GMTKN30 with the Largest Weights (MB08-165, W4-08, BH76, BSR36, S22, and CYCONF)

	WTMAD Error (kcal/mol)		
basis set	PBE0-DH	PBE0-2	QACF-2
def2-TZVPP	4.08	2.50	3.45
def2-QZVP	3.88	2.24	2.87

Higher-Order Effects. Although the performance of simple quadratic adiabatic connection is very promising without introducing fitting parameters, we assessed the effects of higher-order correction terms on the chemical accuracy to further validate (or correct) QACF-2. To this end, we used eq 16 and performed the global optimization for the set of (c_0, c_1, c_2) parameters by thoroughly scanning the three-dimensional (3-D) parameter space defined by (−0.1, −0.1, −0.1) and (0.1, 0.1, 0.1), as shown in Figure 3. Since the results are visually shown in Figure 3, the optimal higher-order parameters are calculated to be (c_0, c_1, c_2) = (−0.0160, 0.004, 0.0550), which is very close to the quadratic origin, with the WTMAD error of 1.81 kcal/mol. It means that the QACF-2 (error of 2.35 kcal/mol) is already almost optimal, and the empirical higher-order effects are measured as 0.54 kcal/mol. To improve the accuracy even further, one may find a better approximation to W_1^{DFA} than PBE as used here, perhaps as a linear combination of LDA and various GGA components. Or one can consider a linear combination of LDA, GGA, or PT2 terms as a higher-order contribution. Perhaps the latter aspects (better approximation to W_1^{DFA}, as well as inclusion of higher-order effects via empirical fitting) are the origin of slightly improved performance of XYG3 and other empirically fitted DHDFs.

Nonlocal Expansion Coefficients. The expansion coefficients derived in eq 14 are noteworthy. Since the nonlocal contributions are of interest, we compared the coefficients of nonlocal terms in Table 3. Note that, interestingly, the HF-exchange and PT2 coefficients in most existing DHDFs fitted numerically for real systems typically lie on the interval [0.50, 0.80] and [0.25, 0.50], respectively.[21,33] These empirically optimized parameters are remarkably (or fortuitously) similar among themselves and also to the present coefficients derived based on the quadratic formula. For B2GP-PLYP, these optimized nonlocal coefficients are even almost identical to those of the QACF-2 derivation. This comparison points to an interesting speculation that the quadratic approximation of the adiabatic connection formula might be very close to describing the real form of W_λ.

In the very final stage of the revision of this paper, interestingly, a similar work[55] that utilizes a quadratic adiabatic connection model (denoted as a quadratic integrand double hybrid, QIDH) has appeared in the literature, although it was submitted several months later than the initial version of the present manuscript. The only difference in QIDH is the approximation of W_1 as a linear combination of E_x^{HF}, E_x^{DFA}, and E_c^{DFA} ($xE_x^{HF} + (1 - x)E_x^{DFA} + 2E_c^{DFA}$), where the authors used the LS1DH formula to obtain $a_x = 3^{-1/3} \approx 0.69$. The resulting coefficients are very similar (for QACF-2: a_x = 0.66 and a_c =

dx.doi.org/10.1021/ct500660k | J. Chem. Theory Comput. XXXX, XXX, XXX−XXX

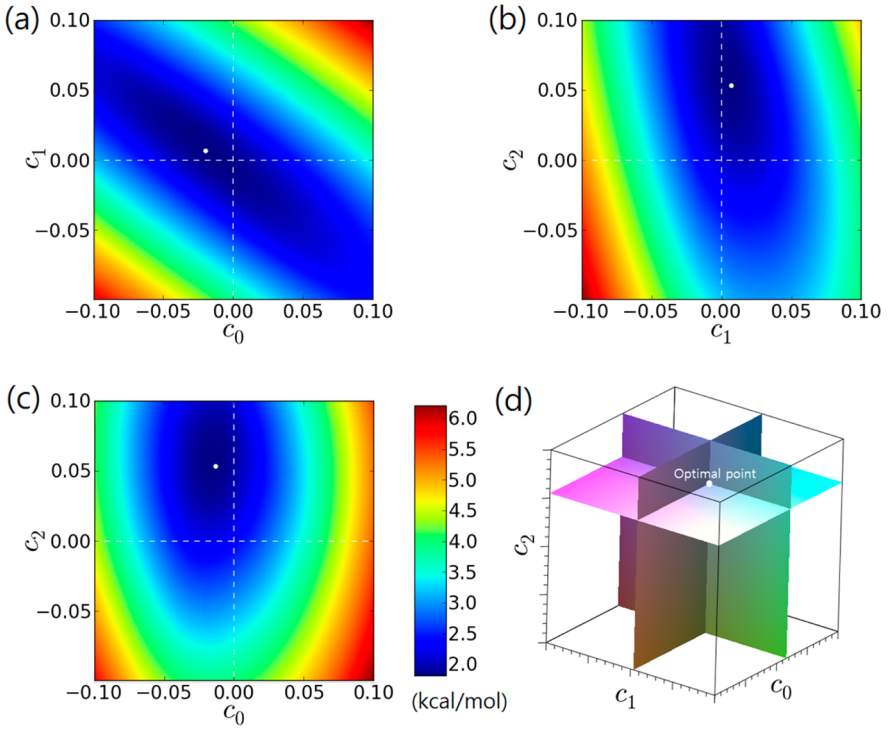

Figure 3. Estimating the higher-order effects of QACF-2 by calculating the WTMAD errors with two adjustable parameters (c_0, c_1), or (c_1, c_2), or (c_0, c_2). All calculations were performed using the 6-311+G(3df,2p) basis. The white dot indicates the location of optimal point in the two-dimensional (2-D) parameter space (or the space that represents the higher-order effects). In the three-dimensional (3-D) box shown in the lower right corner, the point of intersection is the optimal point.

Table 3. Expansion Coefficients for the Nonlocal Terms (a_{HF} = Hartree-Fock Exchange; a_{PT2} = PT2 Correlation) in Various Empirically Optimized DHDFs, in Comparison with Those of QACF-2

functional	a_{HF}	a_{PT2}
B2PLYP (ref 15)	0.53	0.27
B2T-PLYP (ref 18)	0.60	0.31
B2K-PLYP (ref 18)	0.72	0.42
B2GP-PLYP (ref 33)	0.65	0.36
B2−P3LYP (ref 17)	0.53	0.27
XYG3 (ref 20)	0.80	0.32
QACF-2 (present work)	0.67	0.33
average	0.64	0.33

0.33; for QIDH: a_x = 0.69 and a_c = 0.33). For the six representative subsets of GMTKN30 that we used above for the basis set dependence, the WTMAD for PBE-QIDH is 3.05 kcal/mol, and that for QACF-2 is 2.87 kcal/mol. Perhaps the small difference may be due to the approximation of W_1 or the chosen database for benchmark.

V. CONCLUSION

We derived a general framework for developing density functionals based on the polynomial series expansion of the adiabatic connection function. In particular, we showed that the quadratic approximation to the adiabatic connection, in combination with Goling−Levy perturbation theory (QACF-2), yields a parameter-free double-hybrid functional with an accuracy of 2.35 kcal/mol for the GMTKN30 chemical database. Higher-order effects beyond the quadratic truncation are estimated to be 0.54 kcal/mol, lowering the overall error to 1.81 kcal/mol. The resulting linear expansion coefficients for the nonlocal Hartree−Fock and PT2 terms are a_{HF} = 2/3, a_{PT2} = 1/3, respectively, which are in excellent agreement with many existing highly optimized empirical DHDFs. The exact λ dependence of W_λ is known for only a few systems, such as the H_2 molecule, and will probably remain unknown like exact E_{xc}, but the high accuracy of simple analytical functionals, such as QACF-2, suggests that the quadratic λ-dependence is a promising starting point to exact W_λ.

APPENDIX

This appendix shows how the GGA AC function was implemented into the quantum chemistry package and calculated in this work. The basic idea involves rescaling to the original coordinate via variable substitution and integrating it. The GGA can be generally expressed as

$$E_{xc}^{GGA} = \int d^3r e(\rho_\uparrow(r), \rho_\downarrow(r), \nabla\rho_\uparrow(r), \nabla\rho_\downarrow(r)) \quad \text{(A1)}$$

According to eq 5, the AC function for GGA is, therefore,[44]

$$W_\lambda^{GGA} = \frac{d}{d\lambda}[\lambda^2 \int d^3r e(\lambda^{-3}\rho_\uparrow(r/\lambda), \lambda^{-3}\rho_\downarrow(r/\lambda), \lambda^{-3}\nabla\rho_\uparrow(r/\lambda), \lambda^{-3}\nabla\rho_\downarrow(r/\lambda))]$$
$$= \frac{d}{d\lambda}[\lambda^5 \int d^3r e(\lambda^{-3}\rho_\uparrow(r), \lambda^{-3}\rho_\downarrow(r), \lambda^{-4}\nabla\rho_\uparrow(r), \lambda^{-4}\nabla\rho_\downarrow(r))] \quad \text{(A2)}$$

However, the direct computation of eq A1 is not efficient, since it includes the gradient vector of electron density. The integrand of typical GGA is dependent only on the spin density and the magnitudes of density gradients and their inner product $(\rho_\uparrow,\rho_\downarrow,\sigma_{\uparrow\uparrow} = |\nabla\rho_\uparrow(r)|^2,\sigma_{\downarrow\downarrow} = |\nabla\rho_\downarrow(r)|^2,\sigma_{\uparrow\downarrow} =$

$\nabla\rho_\uparrow(r)\cdot\nabla\rho_\downarrow(r)$). In many quantum chemistry packages, the GGA functional is coded by the form of

$$E_{xc}^{GGA} = \int d^3 r e(\rho_\uparrow, \rho_\downarrow, \sigma_{\uparrow\uparrow}, \sigma_{\downarrow\downarrow}, \sigma_{\uparrow\downarrow}) \tag{A3}$$

With some manipulation, the AC function is then

$$W_\lambda^{GGA} = \frac{d}{d\lambda}[\lambda^5 \int d^3 r e(\lambda^{-3}\rho_\uparrow, \lambda^{-3}\rho_\downarrow, \lambda^{-8}\sigma_{\uparrow\uparrow}, \lambda^{-8}\sigma_{\downarrow\downarrow}, \lambda^{-8}\sigma_{\uparrow\downarrow})] = \lambda^4 \int d^3 r w(\lambda^{-3}\rho_\uparrow, \lambda^{-3}\rho_\downarrow, \lambda^{-8}\sigma_{\uparrow\uparrow}, \lambda^{-8}\sigma_{\downarrow\downarrow}, \lambda^{-8}\sigma_{\uparrow\downarrow}) \tag{A4}$$

$$w(\rho_\uparrow, \rho_\downarrow, \sigma_{\uparrow\uparrow}, \sigma_{\downarrow\downarrow}, \sigma_{\uparrow\downarrow}) = 5e - 3\left(\rho_\uparrow\frac{\partial e}{\partial \rho_\uparrow} + \rho_\downarrow\frac{\partial e}{\partial \rho_\downarrow}\right) - 8\left(\sigma_{\uparrow\uparrow}\frac{\partial e}{\partial \sigma_{\uparrow\uparrow}} + \sigma_{\downarrow\downarrow}\frac{\partial e}{\partial \sigma_{\downarrow\downarrow}} + \sigma_{\uparrow\downarrow}\frac{\partial e}{\partial \sigma_{\uparrow\downarrow}}\right) \tag{A5}$$

The first derivatives for building the effective Hamiltonian matrix can be deduced in a similar way:

$$\frac{\partial}{\partial \rho_i}\lambda^4 w(\lambda^{-3}\rho_\uparrow, \lambda^{-3}\rho_\downarrow, \lambda^{-8}\sigma_{\uparrow\uparrow}, \lambda^{-8}\sigma_{\downarrow\downarrow}, \lambda^{-8}\sigma_{\uparrow\downarrow}) = w_{\rho_i}(\lambda^{-3}\rho_\uparrow, \lambda^{-3}\rho_\downarrow, \lambda^{-8}\sigma_{\uparrow\uparrow}, \lambda^{-8}\sigma_{\downarrow\downarrow}, \lambda^{-8}\sigma_{\uparrow\downarrow}) \tag{A6}$$

$$w_{\rho_i}(\rho_\uparrow, \rho_\downarrow, \sigma_{\uparrow\uparrow}, \sigma_{\downarrow\downarrow}, \sigma_{\uparrow\downarrow}) = \lambda\left[2\frac{\partial e}{\partial \rho_i} - 3\left(\rho_\uparrow\frac{\partial^2 e}{\partial \rho_i \partial \rho_\uparrow} + \rho_\downarrow\frac{\partial^2 e}{\partial \rho_i \partial \rho_\downarrow}\right) - 8\left(\sigma_{\uparrow\uparrow}\frac{\partial^2 e}{\partial \rho_i \partial \sigma_{\uparrow\uparrow}} + \sigma_{\downarrow\downarrow}\frac{\partial^2 e}{\partial \rho_i \partial \sigma_{\downarrow\downarrow}} + \sigma_{\uparrow\downarrow}\frac{\partial^2 e}{\partial \rho_i \partial \sigma_{\uparrow\downarrow}}\right)\right] \tag{A7}$$

$$\frac{\partial}{\partial \sigma_{ij}}\lambda^4 w(\lambda^{-3}\rho_\uparrow, \lambda^{-3}\rho_\downarrow, \lambda^{-8}\sigma_{\uparrow\uparrow}, \lambda^{-8}\sigma_{\downarrow\downarrow}, \lambda^{-8}\sigma_{\uparrow\downarrow}) = w_{\sigma_{ij}}(\lambda^{-3}\rho_\uparrow, \lambda^{-3}\rho_\downarrow, \lambda^{-8}\sigma_{\uparrow\uparrow}, \lambda^{-8}\sigma_{\downarrow\downarrow}, \lambda^{-8}\sigma_{\uparrow\downarrow}) \tag{A8}$$

$$w_{\sigma_{ij}}(\rho_\uparrow, \rho_\downarrow, \sigma_{\uparrow\uparrow}, \sigma_{\downarrow\downarrow}, \sigma_{\uparrow\downarrow}) = \lambda^{-4}\left[-3\frac{\partial e}{\partial \sigma_{ij}} - 3\left(\rho_\uparrow\frac{\partial^2 e}{\partial \sigma_{ij} \partial \rho_\uparrow} + \rho_\downarrow\frac{\partial^2 e}{\partial \sigma_{ij} \partial \rho_\downarrow}\right) - 8\left(\sigma_{\uparrow\uparrow}\frac{\partial^2 e}{\partial \sigma_{ij} \partial \sigma_{\uparrow\uparrow}} + \sigma_{\downarrow\downarrow}\frac{\partial^2 e}{\partial \sigma_{ij} \partial \sigma_{\downarrow\downarrow}} + \sigma_{\uparrow\downarrow}\frac{\partial^2 e}{\partial \sigma_{ij} \partial \sigma_{\uparrow\downarrow}}\right)\right] \tag{A9}$$

AUTHOR INFORMATION

Corresponding Author

*E-mail: ysjn@kaist.ac.kr.

Notes

The authors declare no competing financial interest.

ACKNOWLEDGMENTS

This research is supported by the National Research Foundation of Korea (2014R1A4A1003712, 2012-M3C1A6035359, 2012-C1AAA001-M1A2A2026588). We acknowledge the generous supercomputing time from KISTI.

REFERENCES

(1) Kohn, W.; Sham, L. Self-Consistent Equations Including Exchange and Correlation Effects. *Phys. Rev.* **1965**, *140*, 1133−1138.

(2) Hohenberg, P.; Kohn, W. Inhomogeneous Electron Gas. *Phys. Rev.* **1964**, *136*, B864.

(3) Jung, Y.; Head-Gordon, M. What Is the Nature of the Long Bond in the TCNE22−Π-Dimer? *Phys. Chem. Chem. Phys.* **2004**, *6*, 2008−2011.

(4) Becke, A. A New Mixing of Hartree−Fock and Local Density-Functional Theories. *J. Chem. Phys.* **1993**, *98*, 1372.

(5) Langreth, D.; Perdew, J. The Exchange-Correlation Energy of a Metalic Surface. *Solid State Commun.* **1975**, *17*, 1425.

(6) Gunnarsson, O.; Lundqvist, B. Exchange and Correlation in Atoms, Molecules, and Solids by the Spin-Density-Functional Formalism. *Phys. Rev. B* **1976**, *13*, 4274−4298.

(7) Langreth, D.; Perdew, J. Exchange-Correlation Energy of a Metallic Surface: Wave-Vector Analysis. *Phys. Rev. B* **1977**, *15*, 2884.

(8) Perdew, J.; Wang, Y. Accurate and Simple Analytic Representation of the Electron-Gas Correlation Energy. *Phys. Rev. B* **1992**, *45*, 244−249.

(9) Levy, M.; Perdew, J. P. Hellmann−Feynman, Virial, and Scaling Requisites for the Exact Universal Density Functionals. Shape of the Correlation Potential and Diamagnetic Susceptibility for Atoms. *Phys. Rev. A* **1985**, *32*, 2010.

(10) Levy, M.; Yang, W.; Parr, R. G. A New Functional with Homogeneous Coordinate Scaling in Density Functional Theory: $F[P,\lambda]$. *J. Chem. Phys.* **1985**, *83*, 2334.

(11) Perdew, J. P.; Ernzerhof, M.; Burke, K. Rationale for Mixing Exact Exchange with Density Functional Approximations. *J. Chem. Phys.* **1996**, *105*, 9982.

(12) Burke, K.; Ernzerhof, M.; Perdew, J. The Adiabatic Connection Method: A Non-Empirical Hybrid. *Chem. Phys. Lett.* **1997**, *265*, 115−120.

(13) Mori-Sánchez, P.; Cohen, A. J.; Yang, W. Self-Interaction-Free Exchange-Correlation Functional for Thermochemistry and Kinetics. *J. Chem. Phys.* **2006**, *124*, 91102.

(14) Zhao, Y.; Lynch, B. J.; Truhlar, D. G. Doubly Hybrid Meta DFT: New Multi-Coefficient Correlation and Density Functional Methods for Thermochemistry and Thermochemical Kinetics. *J. Phys. Chem. A* **2004**, *108*, 4786−4791.

(15) Grimme, S. Semiempirical Hybrid Density Functional with Perturbative Second-Order Correlation. *J. Chem. Phys.* **2006**, *124*, 034108.

(16) Schwabe, T.; Grimme, S. Double-Hybrid Density Functionals with Long-Range Dispersion Corrections: Higher Accuracy and Extended Applicability. *Phys. Chem. Chem. Phys.* **2007**, *9*, 3397−3406.

(17) Benighaus, T.; DiStasio, R. A.; Lochan, R. C.; Chai, J.-D.; Head-Gordon, M. Semiempirical Double-Hybrid Density Functional with Improved Description of Long-Range Correlation. *J. Phys. Chem. A* **2008**, *112*, 2702−2712.

(18) Tarnopolsky, A.; Karton, A.; Sertchook, R.; Vuzman, D.; Martin, J. M. L. Double-Hybrid Functionals for Thermochemical Kinetics. *J. Phys. Chem. A* **2008**, *112*, 3−8.

(19) Chai, J.-D.; Head-Gordon, M. Long-Range Corrected Double-Hybrid Density Functionals. *J. Chem. Phys.* **2009**, *131*, 174105.

(20) Zhang, Y.; Xu, X.; Goddard, W. A. Doubly Hybrid Density Functional for Accurate Descriptions of Nonbond Interactions, Thermochemistry, and Thermochemical Kinetics. *Proc. Natl. Acad. Sci. U. S. A.* **2009**, *106*, 4963−4968.

(21) Brémond, E.; Adamo, C. Seeking for Parameter-Free Double-Hybrid Functionals: The PBE0-DH Model. *J. Chem. Phys.* **2011**, *135*, 024106.

(22) Fromager, E. Rigorous Formulation of Two-Parameter Double-Hybrid Density-Functionals. *J. Chem. Phys.* **2011**, *135*, 244106.

(23) Kozuch, S.; Martin, J. M. L. DSD-PBEP86: In Search of the Best Double-Hybrid DFT with Spin-Component Scaled MP2 and Dispersion Corrections. *Phys. Chem. Chem. Phys.* **2011**, *13*, 20104−20107.

(24) Sharkas, K.; Toulouse, J.; Savin, A. Double-Hybrid Density-Functional Theory Made Rigorous. *J. Chem. Phys.* **2011**, *134*, 064113.

(25) Toulouse, J.; Sharkas, K.; Brémond, E.; Adamo, C. Communication: Rationale for a New Class of Double-Hybrid Approximations in Density-Functional Theory. *J. Chem. Phys.* **2011**, *135*, 101102.

(26) Zhang, I. Y.; Xu, X.; Jung, Y.; Goddard, W. A. A Fast Doubly Hybrid Density Functional Method Close to Chemical Accuracy Using a Local Opposite Spin Ansatz. *Proc. Natl. Acad. Sci. U. S. A.* **2011**, *108*, 19896−19900.
(27) Chai, J.-D.; Mao, S.-P. Seeking for Reliable Double-Hybrid Density Functionals without Fitting Parameters: The PBE0−2 Functional. *Chem. Phys. Lett.* **2012**, *538*, 121−125.
(28) Zhang, I. Y.; Su, N. Q.; Brémond, É. A. G.; Adamo, C.; Xu, X. Doubly Hybrid Density Functional *x*DH-PBE0 from a Parameter-Free Global Hybrid Model PBE0. *J. Chem. Phys.* **2012**, *136*, 174103.
(29) Aragó, J.; Ortí, E.; Sancho-García, J. C. Nonlocal van Der Waals Approach Merged with Double-Hybrid Density Functionals: Toward the Accurate Treatment of Noncovalent Interactions. *J. Chem. Theory Comput.* **2013**, *9*, 3437−3443.
(30) Peverati, R.; Head-Gordon, M. Orbital Optimized Double-Hybrid Density Functionals. *J. Chem. Phys.* **2013**, *139*, 024110.
(31) Su, N. Q.; Xu, X. Construction of a Parameter-Free Doubly Hybrid Density Functional from Adiabatic Connection. *J. Chem. Phys.* **2014**, *140*, 18A512.
(32) Kozuch, S.; Martin, J. M. L. Spin-Component-Scaled Double Hybrids: An Extensive Search for the Best Fifth-Rung Functionals Blending DFT and Perturbation Theory. *J. Comput. Chem.* **2013**, *34*, 2327−2344.
(33) Karton, A.; Tarnopolsky, A.; Lamère, J.-F.; Schatz, G. C.; Martin, J. M. L. Highly Accurate First-Principles Benchmark Data Sets for the Parametrization and Validation of Density Functional and Other Approximate Methods. Derivation of a Robust, Generally Applicable, Double-Hybrid Functional for Thermochemistry and Thermochemical. *J. Phys. Chem. A* **2008**, *112*, 12868−12886.
(34) Kozuch, S.; Gruzman, D.; Martin, J. M. L. DSD-BLYP: A General Purpose Double Hybrid Density Functional Including Spin Component Scaling and Dispersion Correction. *J. Phys. Chem. C* **2010**, *114*, 20801−20808.
(35) Schwabe, T.; Grimme, S. Double-Hybrid Density Functionals with Long-Range Dispersion Corrections: Higher Accuracy and Extended Applicability. *Phys. Chem. Chem. Phys.* **2007**, *9*, 3397−3406.
(36) Goerigk, L.; Grimme, S. A Thorough Benchmark of Density Functional Methods for General Main Group Thermochemistry, Kinetics, and Noncovalent Interactions. *Phys. Chem. Chem. Phys.* **2011**, *13*, 6670−6688.
(37) Grimme, S. Improved Second-Order Møller−Plesset Perturbation Theory by Separate Scaling of Parallel- and Antiparallel-Spin Pair Correlation Energies. *J. Chem. Phys.* **2003**, *118*, 9095.
(38) Görling, A.; Levy, M. Exact Kohn−Sham Scheme Based on Perturbation Theory. *Phys. Rev. A* **1994**, *50*, 196.
(39) Goerigk, L.; Grimme, S. Efficient and Accurate Double-Hybrid-Meta-GGA Density Functionals Evaluation with the Extended GMTKN30 Database for General Main Group Thermochemistry, Kinetics, and Noncovalent Interactions. *J. Chem. Theory Comput.* **2011**, *7*, 291−309.
(40) Peach, M. J. G.; Miller, A. M.; Teale, A. M.; Tozer, D. J. Adiabatic Connection Forms in Density Functional Theory: H_2 and the He Isoelectronic Series. *J. Chem. Phys.* **2008**, *129*, 064105.
(41) Cohen, A. J.; Mori-Sánchez, P.; Yang, W. Assessment and Formal Properties of Exchange-Correlation Functionals Constructed from the Adiabatic Connection. *J. Chem. Phys.* **2007**, *127*, 034101.
(42) Teale, A. M.; Coriani, S.; Helgaker, T. Accurate Calculation and Modeling of the Adiabatic Connection in Density Functional Theory. *J. Chem. Phys.* **2010**, *132*, 164115.
(43) Adamo, C.; Barone, V. Toward Reliable Adiabatic Connection Models Free from Adjustable Parameters. *Chem. Phys. Lett.* **1997**, *274*, 242−250.
(44) Ernzerhof, M. Construction of the Adiabatic Connection. *Chem. Phys. Lett.* **1996**, *4*, 13−17.
(45) Peach, M. J. G.; Teale, A. M.; Tozer, D. J. Modeling the Adiabatic Connection in H_2. *J. Chem. Phys.* **2007**, *126*, 244104.
(46) Seidl, M.; Perdew, J.; Kurth, S. Simulation of All-Order Density-Functional Perturbation Theory, Using the Second Order and the Strong-Correlation Limit. *Phys. Rev. Lett.* **2000**, *84*, 5070−5073.
(47) Pinkus, A. Weierstrass and Approximation Theory. *J. Approx. Theory* **2000**, *107*, 1−66.
(48) Lubinsky, D. Weierstrass' Theorem in the Twentieth Century: A Selection. *Quaest. Math.* **1995**, *18*, 91−130.
(49) Goerigk, L.; Grimme, S. A General Database for Main Group Thermochemistry, Kinetics, and Noncovalent Interactions—Assessment of Common and Reparameterized (meta-) GGA Density. *J. Chem. Theory Comput.* **2009**, *6*, 107−126.
(50) Shao, Y.; Molnar, L. F.; Jung, Y.; Kussmann, J.; Ochsenfeld, C.; Brown, S. T.; Gilbert, A. T. B.; Slipchenko, L. V.; Levchenko, S. V.; O'Neill, D. P.; DiStasio, R. A.; Lochan, R. C.; Wang, T.; Beran, G. J. O.; Besley, N. A.; Herbert, J. M.; Lin, C. Y.; Van Voorhis, T.; Chien, S. H.; Sodt, A.; Steele, R. P.; Rassolov, V. A.; Maslen, P. E.; Korambath, P. P.; Adamson, R. D.; Austin, B.; Baker, J.; Byrd, E. F. C.; Dachsel, H.; Doerksen, R. J.; Dreuw, A.; Dunietz, B. D.; Dutoi, A. D.; Furlani, T. R.; Gwaltney, S. R.; Heyden, A.; Hirata, S.; Hsu, C.-P.; Kedziora, G.; Khalliulin, R. Z.; Klunzinger, P.; Lee, A. M.; Lee, M. S.; Liang, W.; Lotan, I.; Nair, N.; Peters, B.; Proynov, E. I.; Pieniazek, P. A.; Rhee, Y. M.; Ritchie, J.; Rosta, E.; Sherrill, C. D.; Simmonett, A. C.; Subotnik, J. E.; Woodcock, H. L.; Zhang, W.; Bell, A. T.; Chakraborty, A. K.; Chipman, D. M.; Keil, F. J.; Warshel, A.; Hehre, W. J.; Schaefer, H. F.; Kong, J.; Krylov, A. I.; Gill, P. M. W.; Head-Gordon, M. Advances in Methods and Algorithms in a Modern Quantum Chemistry Program Package. *Phys. Chem. Chem. Phys.* **2006**, *8*, 3172−3191.
(51) Řezáč, J.; Riley, K. E.; Hobza, P. S66: A Well-Balanced Database of Benchmark Interaction Energies Relevant to Biomolecular Structures. *J. Chem. Theory Comput.* **2011**, *7*, 2427.
(52) Wolinski, K.; Pulay, P. Second-Order Møller−Plesset Calculations with Dual Basis Sets. *J. Chem. Phys.* **2003**, *118*, 9497.
(53) Zhang, I. Y.; Luo, Y.; Xu, X. Basis Set Dependence of the Doubly Hybrid XYG3 Functional. *J. Chem. Phys.* **2010**, *133*, 104105.
(54) Zhang, I. Y.; Luo, Y.; Xu, X. XYG3s: Speedup of the XYG3 Fifth-Rung Density Functional with Scaling-All-Correlation Method. *J. Chem. Phys.* **2010**, *132*, 194105.
(55) Brémond, É.; Sancho-García, J. C.; Pérez-Jiménez, Á. J.; Adamo, C. Communication: Double-Hybrid Functionals from Adiabatic-Connection: The QIDH Model. *J. Chem. Phys.* **2014**, *031101*, 141.